

Strathprints Institutional Repository

Lee, Yongwon and Chan, Hoi-Sang and Pu, Yongchang and Incecik, Atilla and Dow, Robert S. (2012) *Global wave loads on a damaged ship*. *Ships and Offshore Structures*, 7 (3). pp. 237-268. ISSN 1744-5302

Strathprints is designed to allow users to access the research output of the University of Strathclyde. Copyright © and Moral Rights for the papers on this site are retained by the individual authors and/or other copyright owners. You may not engage in further distribution of the material for any profitmaking activities or any commercial gain. You may freely distribute both the url (<http://strathprints.strath.ac.uk/>) and the content of this paper for research or study, educational, or not-for-profit purposes without prior permission or charge.

Any correspondence concerning this service should be sent to Strathprints administrator: <mailto:strathprints@strath.ac.uk>

Global Wave Loads on a Damaged Ship

Yongwon Lee^{a*}, Hoi-Sang Chan^b, Yongchang Pu^b, Atilla Incecik^c and Robert S. Dow^b

^aMarine Product Development, Lloyd's Register, London, UK; ^bMarine Science and Technology, Newcastle University, Newcastle upon Tyne, UK; ^cNaval Architecture and Marine Engineering, University of Strathclyde, Glasgow, UK

A computational tool was applied based on a two dimensional linear method to predict the hydrodynamic loads for damaged ships. Experimental tests on a ship model have also been carried out to predict the hydrodynamic loads in various design conditions. The results of the theoretical method and experimental tests are compared to validate the theoretical method. The extreme wave-induced loads have been calculated by short term prediction. For the loads in intact condition, the prediction with duration of 20 years at sea state 5 is used, while for loads in damaged conditions the prediction in 96 hours exposure time at sea 3 is used. The maximum values of the most probable extreme amplitudes of dynamic wave induced loads in damaged conditions are much less than those in intact condition because of the reduced time. An opening could change the distribution of not only stillwater bending moment but also wave-induced bending moment. It is observed that although some cross sections are not structurally damaged, the total loads acting on these cross sections after damage may be increased dramatically compared to the original design load in intact condition.

Keywords: damaged ship; flooding; model test; static load; wave induced load; short-term prediction

INTRODUCTION

A large number of ship accidents continue to occur despite the advances with the navigation systems. These accidents would cause the loss of cargos, pollution of environment, even loss of human beings. Based on statistical data of Lloyd's Register of Shipping (Lloyd's Register, 2000), a total of 1336 ships were lost with 6.6 million gross tonnage cargo loss between 1995 and 2000. 2727 people were reported killed or missing as a result of total losses in this period. So it is very important to ensure an acceptable safety level for damaged ships. Unfortunately adequate structural strength in intact condition does not necessarily guarantee an acceptable safety margin in damaged conditions. Conventionally only the structural strength in intact condition was assessed in the design. When a ship is damaged, the operators need to decide the immediate maintenance actions by evaluating the effects of the damage on the safety of the ship using the load prediction procedure and the residual strength assessment procedure for the damaged ship. For that reason the loading changes in the damage should be considered in the design phase.

The prediction of ship motions and dynamic wave induced loads acting on a ship has been a main theme in the field of ship hydrodynamics. The development of a two-dimensional harmonic flow solution was accomplished by Ursell (1949). Korvin-Kroukovsky (1955) introduced the heuristically-derived strip theory to ship motions as the first strip theory. This theory was modified by his sequel paper (Korvin-Kroukovsky and Jacobs, 1957) and Jacobs (1958), and the theory restricted on heaving and pitching only. Jacobs (1960) carried out correlation works with the analytical calculation of ship bending moments and the results of model tests in regular waves. The validity of

the strip theory on a high-speed destroyer hull was shown in (Gerritsma and Beukelman, 1967). Salvesen et al. (1970) expanded the original theory for more general modes of motions and wave headings. Further a number of improved strip theories have been developed. Among them there are rational strip theory (Ogilvie and Tuck, 1969) and unified strip theory (Newman, 1978). Good agreement between strip theory predictions and experimental data has been found for many classes of mono-hull forms (Kim et al., 1980) and twin-hull ships (Lee and Curphey, 1977).

The above works only studied ship motions and dynamic wave loads acting on a ship in intact condition. In the last decade the study on wave induced loads in damage conditions have been accomplished, but fairly limited. The behaviour of the damaged ship in waves is different from that in intact condition, so it could be analysed in time domain rather than in frequency domain (Santos et al., 2002). A nonlinear time-domain simulation method for the prediction of large amplitude motions of a Ro-Ro ship in intact and damaged conditions was introduced by Chan et al. (2002). In this study numerical computations and model tests have been carried out to investigate the dynamic motion responses of Ro-Ro ship Dextra to various wave amplitudes at different wave headings. Chan et al. (2003) also described global wave load predictions on a Ro-Ro ship in intact and damaged condition. In order to evaluate the method used, results of the vertical bending moment, horizontal bending moment and dynamic torsion as well as dynamic shear force were correlated with model test results. Recently six degrees of freedom motion response tests of a Ro-Ro model (completed for EU project DEXTREMEL) have been reported in regular waves for intact and damaged conditions by Korkut et al. (2004). Korkut et al. (2005) reported measurements of global

*Corresponding author: Dr. Yongwon Lee
Lloyd's Register, 71 Fenchurch Street, London EC3M 4BS
E yongwon.lee@lr.org T +44 20 7423 2204

loads acting on a Ro-Ro ship. The stationary model was tested in different wave heights and wave frequencies for the head, beam and stern quartering seas in order to explore the effect of damage and wave heights on the global loads acting on the model. Recently Lee et al. (2005) has introduced the framework for damage survivability assessment system that can evaluate and improve the ship safety. The importance of predicting accurate wave induced loads and residual strength in a damaged ship was mentioned.

When a ship is in damaged condition its floating condition could be changed dramatically. Its draught is increased and it may heel. It could also have large holes in the structure. If the methodology used for intact condition is blindly applied to damaged condition, the results could be misleading. Ideally the environmental loads should be calculated together with the assessment of the residual strength of the ship. In another words, a systematic approach should be used for a more accurate assessment of residual strength of a damaged ship. Chan, et al, (2001) have shown that the most critical condition for a damaged Ro-Ro ship is in quartering seas. Although the vertical bending moment in quartering seas is smaller than that in head seas, the horizontal bending moment is quite large. The ratio of horizontal bending moment to vertical bending moment could be as large as 1.73. So the combined effect of vertical bending moment and horizontal bending moment is more serious. In addition, torsion, which is not considered in the above study, normally reaches maximum in quartering seas. So the effect of horizontal bending moment and torsion on the ultimate hull girder strength should be considered in the assessment of the safety level of damaged ships.

If a ship is asymmetrically flooded, some effects resulting from heel could be monitored and should be examined. However the previous works carried out by a number of investigators did not consider the asymmetric situations on damaged ships. This means that the vessel has to be always modelled and analysed in the upright condition without heel. For that reason a series of internal seakeeping and loading prediction programmes, UNEW Hydro Programme set, has been developed using two dimensional linear and non-linear strip theory. The two dimensional linear suit aims at helping the operators to decide the immediate maintenance actions by evaluating the effects of the damage and at providing acceptable predictions compared to those of a time domain simulation method. Chan et al. (2003) presented wave induced load predictions with experimental results on a damaged Ro-Ro ship using a non-linear time domain simulation method. But they did not provide more accurate results compared to those of the present linear strip method, although they applied to a more complicated time domain non-linear method. The objective of the research project is to develop a reliability-based procedure to assess the safety level of damaged ships. This paper presents the prediction of the total loads including stillwater bending moment and wave-induced loads for a sample vessel in intact condition and damage conditions. The sample vessel was initially designed by NSWCCD. A general arrangement design and compartment modelling were conducted by the authors. The two dimensional linear analysis was carried out in several design conditions that are intended as examples of ship-ship collision and raking events

as well as intact condition. Experimental study is also carried out to compare the results obtained from the predictions with those obtained from measurements.

METHODOLOGIES

Methodologies for Wave-Induced Loading

A linear two-dimensional strip theory has been developed to predict the wave-induced motions and loads for both intact and damaged conditions. The details are briefly described below. Under the assumptions that the responses are linear and harmonic, the equation of motions of a vessel in regular waves can be written in the following general equation of coupled motions.

$$\sum_{k=1}^6 [(M_{jk} + A_{jk}) \cdot \ddot{\eta}_k + B_{jk} \cdot \dot{\eta}_k + C_{jk} \cdot \eta_k] = E_j \cdot e^{-i\omega t} \quad (1)$$

where:

M_{jk} is the components of the generalised mass matrix

A_{jk} and B_{jk} are matrixes of the added mass and damping coefficients

C_{jk} is the matrix of hydrostatic coefficients

E_j is the complex amplitudes of exciting forces and moments

j and k indicate the direction of fluid force and the modes of motion

(j and k = 1-surge, 2-sway, 3-heave, 4-roll, 5-pitch, 6-yaw)

The derivations of the equation of motions and their components can be found in (Salvesen et al., 1970). However, the motions in vertical and horizontal planes are coupled to each other in asymmetric damaged conditions. Within the framework of linearised potential flow theory, hydrodynamic coefficients and forces were calculated (Chan, 1992). In this study, rigid body motions are considered. The elasticity of the hull girder is assumed to have the insignificant effect on wave induced loads (Adegeest, 1995). To describe wave and ship motions, two sets coordinate systems are considered (see Figure 1). One frame is a right handed coordinate system, which translates with the ship with its origin at the longitudinal centre of gravity (G-xyz). Another coordinate system is the space fixed frame (O-XYZ) as shown in Figure 1, OXY is in the plane of the undisturbed free surface. The vessel is considered to undergo six degree of freedom oscillations about its mean position. These oscillations are better known as surge, sway and heave for translatory oscillations (η_1 , η_2 , and η_3), and roll, pitch and yaw for angular oscillations (η_4 , η_5 , and η_6). Figure 2 shows the definition of wave heading angle (β).

Frank (1967) introduced a method in which the required velocity potential is represented by the distribution of the sources over the submersed cross section. The unknown function of the density of the sources along the cylinder contour is determined from the integral equations obtained by satisfying the kinematic boundary condition over the submersed cross section. The hydrodynamic pressures are obtained from velocity potential by using the linearised Bernoulli Equation. Integration of these pressures over the immersed portion of the cylinder yields the

hydrodynamic forces and moments (Frank, 1967; Chan, et al, 2003). For the calculation of loads due to waves, two-dimensional linear strip theory was used to predict the dynamic loads in the linear frequency domain. It should be noted that this theory does not take into account the flow of water in and out of the damaged compartments. Therefore the sloshing effects of the sea water in the damaged compartments are neglected during the numerical predictions.

By neglecting loads due to slamming and springing, in vertical plane the dynamic loads at each section can be written as the following equation.

$$\begin{aligned} \frac{dF_3}{dx} = & (A_{33}(x) + M(x))\ddot{\eta}_3 + B_{33}(x)\dot{\eta}_3 + C_{33}(x)\eta_3 + A_{32}(x)\ddot{\eta}_2 + B_{32}(x)\dot{\eta}_2 \\ & + A_{34}(x)\ddot{\eta}_4 + B_{34}(x)\dot{\eta}_4 + A_{35}(x)\ddot{\eta}_5 + B_{35}(x)\dot{\eta}_5 + C_{35}(x)\eta_5 - \frac{dE_3}{dx} \end{aligned} \quad (2)$$

The distribution of vertical shear-forces over the length of ship is determined by integration of $\frac{dF_3}{dx}$, and then the distribution of vertical bending moments can be obtained by integrating the shear-forces over the length.

In horizontal plane, the dynamic loads consist of horizontal dynamic loads and torsion moments. These equations can be written as the following forms.

$$\begin{aligned} \frac{dF_2}{dx} = & (A_{22}(x) + M(x))\ddot{\eta}_2 + B_{22}(x)\dot{\eta}_2 + A_{23}(x)\ddot{\eta}_3 + B_{23}(x)\dot{\eta}_3 \\ & + (A_{24}(x) - M(x)z_c)(x)\ddot{\eta}_4 + B_{24}(x)\dot{\eta}_4 + A_{25}(x)\ddot{\eta}_5 + B_{25}(x)\dot{\eta}_5 \\ & + A_{26}(x)\ddot{\eta}_6 + B_{26}(x)\dot{\eta}_6 - \frac{dE_2}{dx} \end{aligned} \quad (3)$$

$$\begin{aligned} \frac{dF_4}{dx} = & (A_{42}(x) - M(x)z_c)\ddot{\eta}_2 + B_{42}(x)\dot{\eta}_2 + (A_{44}(x) + I_4(x))\ddot{\eta}_4 \\ & + A_{43}(x)\ddot{\eta}_3 + B_{43}(x)\dot{\eta}_3 + B_{44}(x)\dot{\eta}_4 + C_{44}(x)\eta_4 + A_{45}(x)\ddot{\eta}_5 \\ & + B_{45}(x)\dot{\eta}_5 + (A_{46}(x) - I_{46}(x))\ddot{\eta}_6 + B_{46}(x)\dot{\eta}_6 - \frac{dE_4}{dx} \end{aligned} \quad (4)$$

Similar treatment with the vertical plane, the distribution of horizontal shear-forces over the length of ship is defined by integration of $\frac{dF_2}{dx}$, while the distribution of horizontal bending moment is obtained by integrating the shear-forces along the length. In the equation (4) z_c stands for the vertical centre of gravity.

Since the equations of motions are linear and harmonic, in which the exciting forces and moments can be written in complex terms, these equations are solved using complex response method. This means that the exciting forces and the responses can be represented as real and imaginary parts. The solutions are then in the forms of amplitudes and their phase-lags (Jacobs et al., 1960; Brebbia, 1979).

Nomenclature

A_{jk} = matrix of added mass coefficients
 Ax = maximum section area
 B = moulded breadth
 B_{jk} = matrix of damping coefficients
 C_B = block coefficient
 C_{jk} = matrix of hydrostatic coefficients
 C_M = midship section coefficient
 C_P = prismatic coefficient
 D = depth to public spaces deck
 E_j = complex amplitude of exciting forces and moments
 FSc = free surface correction
 Fy = horizontal shear force
 Fz = vertical shear force
 $\frac{dF_2}{dx}$ = distribution of horizontal shear-forces over the length of ship
 $\frac{dF_3}{dx}$ = distribution of vertical shear-forces over the length of ship
 GM = metacentric height
 KG = height of centre of gravity
 KM = height of metacentre
 LCG = longitudinal centre of gravity
 L_{oa} = overall length

L_{pp} = length between perpendiculars
 M_{jk} = components of generalised mass matrix
 Mx = torsional moment
 My = vertical bending moment
 Mz = horizontal bending moment
 $SWBM$ = still water bending moment
 T = design draft
 $T(s)$ = wave period
 $WHBM$ = wave-induced horizontal bending moment
 WTM = wave-induced torsional moment
 $WVBM$ = wave-induced vertical bending moment
 j, k = indicates varying from 1 to 6:
1=surge, 2=sway, 3=heave, 4=roll, 5=pitch, 6=yaw
 k_{xx} = roll radius of gyration
 k_{yy} = pitch radius of gyration
 k_{zz} = yaw radius of gyration
 z_c = vertical centre of gravity
 ∇ = volume displacement
 β = wave heading angle
 $\eta_1, \eta_2,$ and η_3 = surge, sway and heave for translatory oscillations
 $\eta_4, \eta_5,$ and η_6 = roll, pitch and yaw for angular oscillations
 $\lambda (m)$ = wave length
 $\omega (r/s)$ = circular frequency

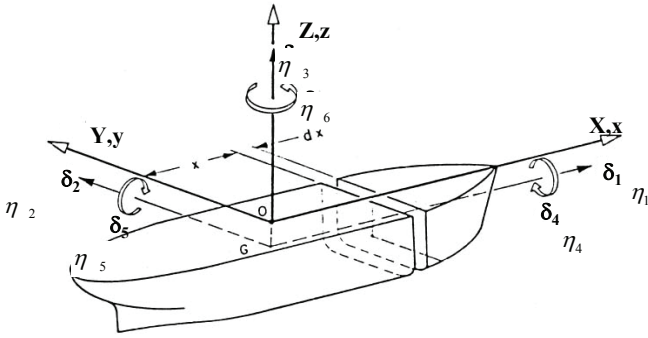


Figure 1: Co-ordinate systems and modes of motions

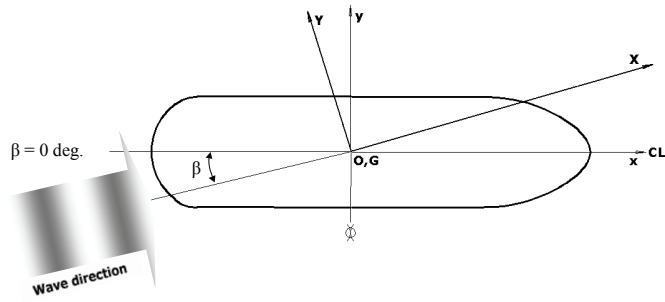


Figure 2: Definition of wave heading

Experimental investigation

The experiments have been carried out at the Newcastle University Towing Tank using a model with a scale of 1/100 of a Notional US Navy Destroyer Hull 5415. The tests measured 6 degree of freedom motion responses of the stationary model without forward speed, as well as global loads in intact and damaged conditions for different headings in regular waves.

Description of the facility and equipment used

The towing tank is 37 metres long, 4 metres wide and has a water depth of 1.2 metres. For the present experimental programme, waves were generated by twelve rolling seal hinged paddle type wave makers normally operating in unison and driven by a sinusoidal source at the desired period and amplitude. The wave makers employ velocity feedback within the electronic control system to stabilise operation and to obtain the desired transfer function, additionally the wave makers incorporate absorption facilities to remove the effects of reflected waves. The wave height and period were monitored and recorded using three Churchill resistance probes and an associated monitor. The probe consists of two parallel wires rigidly separated at both ends with the probe being partially immersed, high frequency current is passed through the wires, the magnitude of which is proportional to the depth of immersion. Thus the changing current is analogous to the wave height.

The six degree of freedom motions of the model were measured using QUALISIS motion capture system. It is

comprised of four infra emitters strategically placed on the vessel. The co-ordinates in the vertical and horizontal plane are registered by detectors located in two cameras suitably positioned above the vessel. The forces and moments were obtained from a five component force gauge, type 206/5C manufactured by Danish Hydraulic Institute (DHI) with the following specifications: $F_y=F_z=125N$, $M_y=M_z=110Nm$ and $M_x=4.0Nm$. This is comprised of two vertical end pieces joined by four beams, one at each corner, machined from solid aluminium. The beams are strain gauged to obtain F_y , F_z , M_x , M_y and M_z . The force gauge was bolted to two substantial bulkheads mounted in the fore and aft parts of the model and the two sections made waterproof by the provision of a thin membrane across the cut. The gauge was located at 545.43 mm from AP longitudinally and at the centre of the depth to public spaces deck which is 62.83 mm from the base line. Table 1 represents amplifier connections and calibration details. A close photograph of the force gauge is given in Figure 3. The convention for the measured loads is described in Figure 4.

Construction of model

The model was made from fibreglass based on the offsets of a sample vessel of Notional US Navy Destroyer Hull 5415. The main particulars of the model are given in Table 2, while the views of the body plan and the model are respectively shown in Figures 5 and 6. As the model was to be tested in damaged conditions as well as in intact condition, an appropriate damage size had to be decided. A two-compartment damage scenario was assumed and the model was damaged at the starboard side in midship area. And a sonar zone damage case at the starboard side in fore body was considered. The details of damaged opening size and location are shown in Figure 7. For the hull girder loading measurements the model used for motion tests was converted. In order to accomplish damaged model tests additional parts were built. $T1 \sim T6$ and $D1 \sim D4$ stand for transverse bulkheads and decks respectively. $L1$ and $L2$ stand for longitudinal girders (see Figure 8).

Table 1: Amplifier connections and calibration details

Fylde amplifier connection	Maximum value	Calibration with gauge clamped to desk	Maximum value
CH1 = F_y	125 N	2.5 kg = 10 volt	24.53 N
CH2 = F_z	125 N	4.0 kg = 10 volt	39.24 N
CH3 = M_y	110 Nm	5.0 kg = 9.81 Nm = 5 volt	19.62 Nm, 200 mm lever
CH4 = M_z	110 Nm	5.0 kg = 9.81 Nm = 10 volt	9.81 Nm, 200 mm lever
CH5 = M_x	4 Nm	2.0 kg = 1.96 Nm = 10 volt	1.96 Nm, 100 mm lever

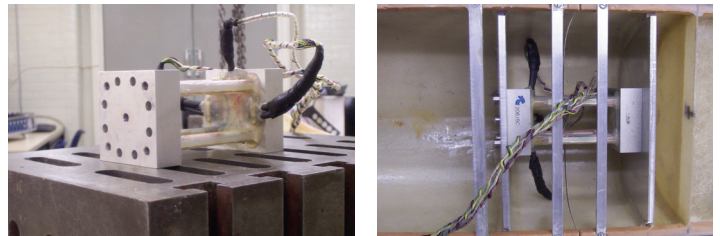


Figure 3: Force gauge installed at AP 545 mm

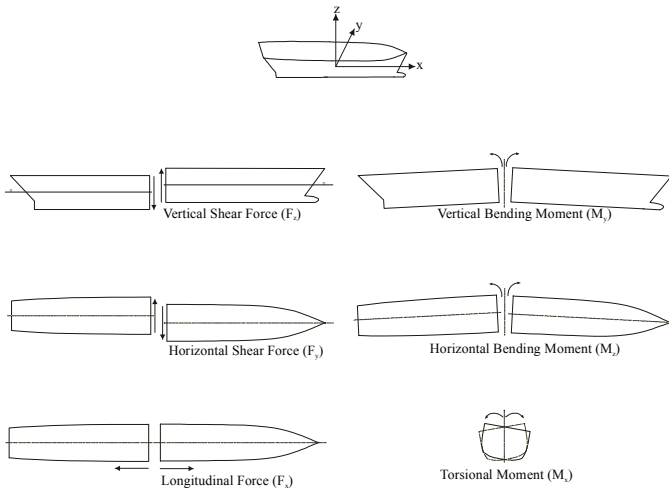


Figure 4: Convention for measured loads

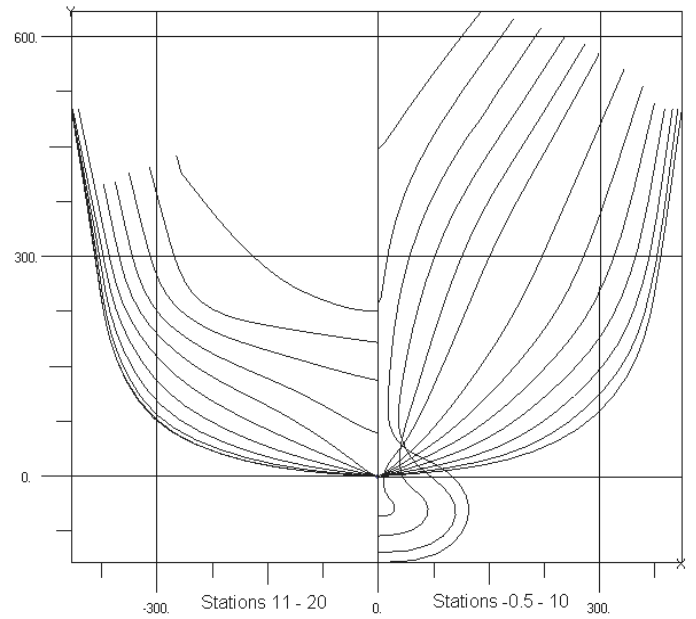


Figure 5: Body plan (Unit: inch)

Table 2: Main particulars of Notional US Navy Destroyer Hull 5415

Particulars	Ship	Model (1/100)
L_{oa} (Length overall) in m	151.1800	1.5118
L_{pp} (Length between perpendiculars) in m	142.0400	1.4204
B (Breadth moulded) in m	20.0300	0.2003
D (Depth to public spaces deck) in m	12.7400	0.1274
T (Design draft) in m	6.3100	0.0631
∇ (Volume) in m^3	8811.9415	0.0088
A_x (Maximum section area) in m^2	96.7923	0.0097
C_B (Block coefficient)	0.4909	0.4909
C_P (Prismatic coefficient)	0.6409	0.6409
C_M (Midship section coefficient)	0.7658	0.7658
KM (Height of metacentre above keel) in m	9.4700	0.0947
KG (Height of centre of gravity above keel) in m	6.2830	0.0628
GM (Metacentric height) in m	3.1870	0.0316
LCG (Longitudinal position CoG from A.P.) in m	71.0200	0.7105
k_{xx} (Roll radius of gyration) in m	-	0.0601
k_{yy} (Pitch radius of gyration) in m	35.5100	0.3363
k_{zz} (Yaw radius of gyration) in m	35.5100	0.3363

Adjustment of centre of gravity

In order to obtain the longitudinal centre of gravity of the model vessel, the method described by Bhattacharyya (1978) was used. The model was placed on two knife-edges, the first knife sitting on the weighing scales, the second on the floor. Then the longitudinal centre of gravity of the model was determined from a moment balance equation. The longitudinal centre of gravity (LCG) of the model was obtained as 710.5 mm from A.P. An inclining test was carried out to determine the vertical centre of gravity (KG) of the model. This indicated a transverse GM value of 31.6 mm. Based on this value KG was calculated as 62.8 mm above the keel.

Adjustment of radii of gyration

In order to adjust the radii of gyration of the model in pitch, yaw and roll, first the radii of gyration of the model were determined by using appropriate tests. The measured values of pitch radius of gyration (k_{yy}), yaw radius of gyration (k_{zz}) and roll radius of gyration (k_{xx}) are given in Table 2. In order to comply with the required radii of gyration and loading condition some weights were added to the model. Bifilar suspension method was used to obtain the yaw radius of gyration given in Bhattacharyya (1978). By using this method the pitch and yaw radii of gyration of the bare model were obtained as: $k_{yy} = k_{zz} = 336.3$ mm. The roll radius of gyration of the model was found to be $k_{xx} = 60.1$ mm following the method given in Bhattacharyya (1978). In order to satisfy the required draught, weight, LCG , KG and the radii of gyration some weights were added at strategic points.

Description of test conditions and test trials

The stationary model tests were carried out with both intact and damage conditions in head, stern quartering and beam waves. For loading tests the total number of recorded runs was 198. Test trials and identifications are provided in Table 3. Table 4 shows a summary of the experimental wave conditions and the corresponding full-scale conditions used in motion and loading tests. The amplitude of the waves for each run was increased gradually to its maximum to minimise the impact effect of the waves. Once the model has reached the steady state condition then the load and pressure records were taken. As soon as the waves reached the beach at the far end of the towing tank, the recordings were stopped to avoid reflected waves reaching the model. A number of different mooring configurations were tried and applied for the specified headings, this was conducted by a

basis of trial and error as well as former experience until the optimum configuration for each heading was determined.

THE DAMAGE SCENARIOS

In this project, four damage scenarios are proposed and shown in Figures 9 ~ 12.

Table 3: Loading test trials and identifications

Condition	Test ID	Hw	Heading	Wave freq.	Total
Intact	LT-ITS-1 ~ 27	small	3	9	27
	LT-ITL-1 ~ 27	large	3	9	27
DS2	LT-DS2S-1 ~ 45	small	5	9	45
	LT-DS2L-1 ~ 45	large	5	9	45
DS3	LT-DS3S-1 ~ 27	small	3	9	27
	LT-DS3L-1 ~ 27	large	3	9	27
Total					198

Table 4: Experimental wave conditions used in model tests

λ/L	λ (m)		ω (r/s)		T (s)		$H1$		$H2$	
	Model	Ship	Model	Ship	Model	Ship	Model	Ship	Model	Ship
3.347	5.061	506.055	3.490	0.349	1.800	18.003	small	small	large	large
2.645	3.999	399.897	3.926	0.393	1.600	16.004	small	small	large	large
2.171	3.281	328.149	4.334	0.433	1.450	14.497	small	small	large	large
1.882	2.845	284.452	4.655	0.466	1.350	13.498	small	small	large	large
1.032	1.560	156.041	6.285	0.629	1.000	9.997	small	small	large	large
0.837	1.265	126.514	6.980	0.698	0.900	9.002	small	small	large	large
0.506	0.764	76.436	8.980	0.898	0.700	6.997	small	small	large	large
0.437	0.661	66.053	9.660	0.966	0.650	6.504	small	small	large	large
0.313	0.473	47.262	11.420	1.142	0.550	5.502	small	small	large	large

where, "small": $(H1)M$ 4.28 ~ 26.35 mm, $(H1)S$ 0.428 ~ 2.635 m

"large": $(H2)M$ 8.39 ~ 45.51 mm, $(H2)S$ 0.839 ~ 4.551 m

λ is the wave length

L is the length between perpendiculars

ω is the wave frequency

T is the wave period

H is the wave height

M and S denote model and ship, respectively.

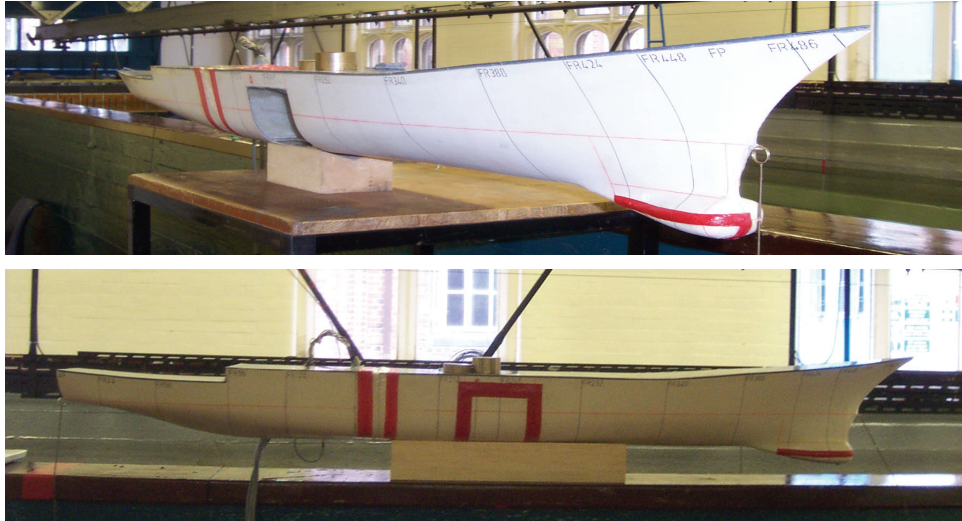


Figure 6: General view of the model

DAMAGED OPENING SIZE AND LOCATION

Unit: Metre, FS: 0.3048 Metre (1 feet), Model Scale: 1/100

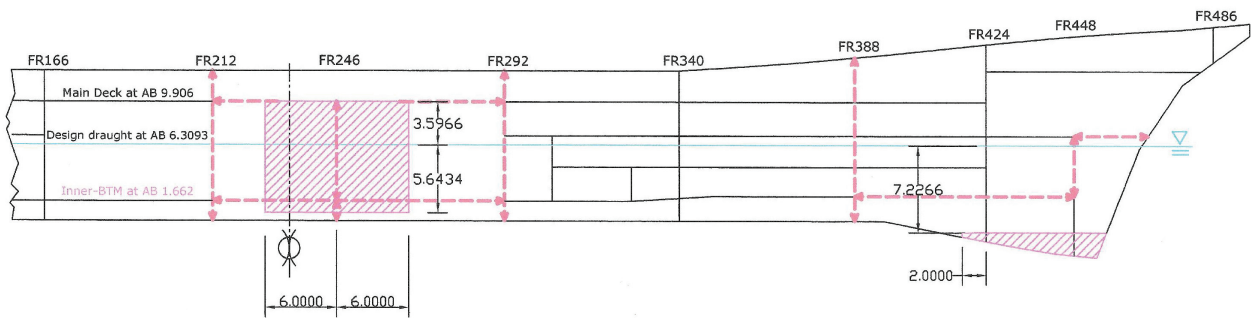


Figure 7: Damaged opening size and location

MODEL COMPARTMENTATION OF H5415

Unit: Metre, FS: 0.3048 Metre (1 feet)

T.BHD: T1 ~ T6, Deck: D1 ~ D4, Long.: L1,L2

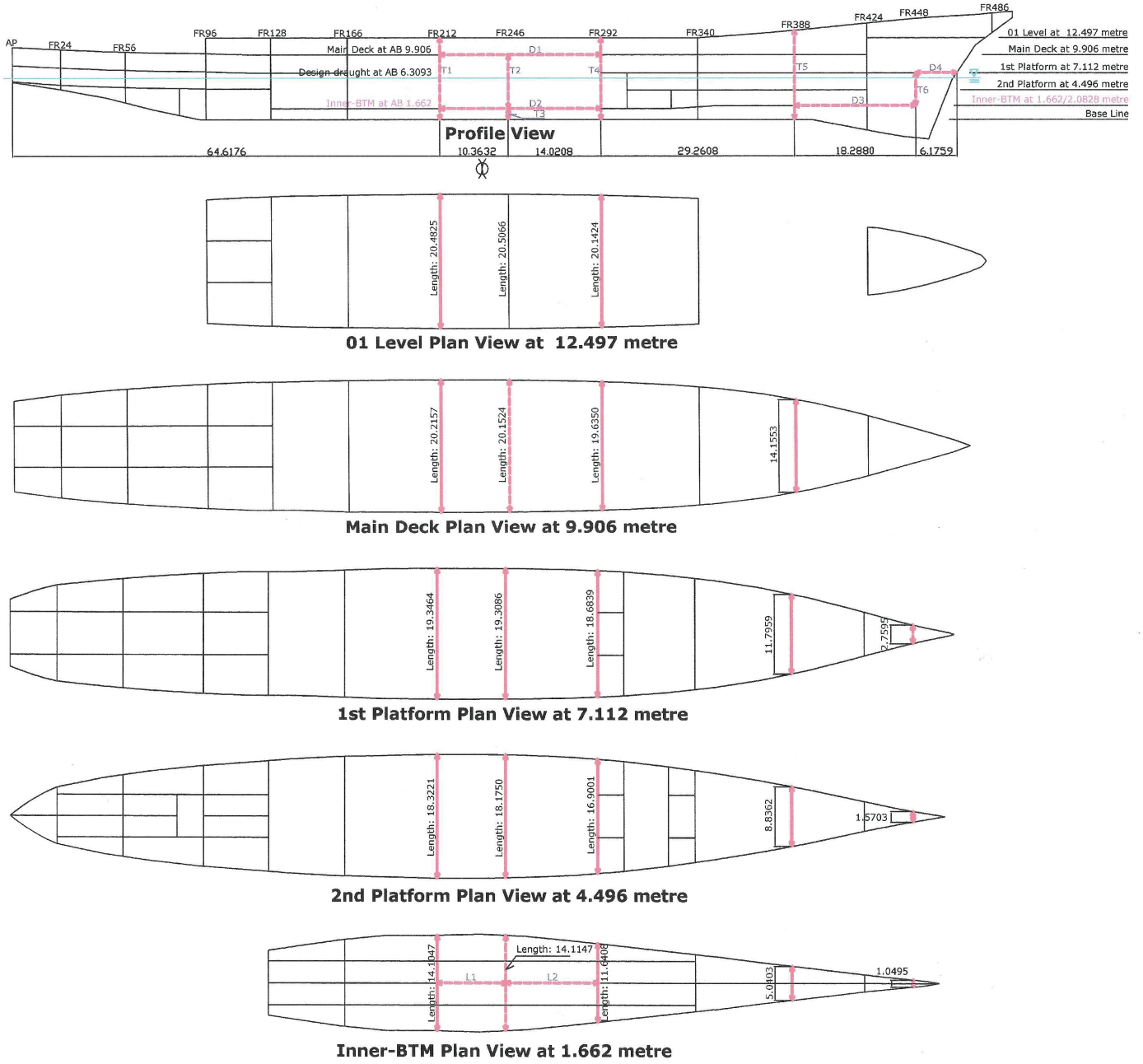


Figure 8: Model compartmentation

DAMAGE SCENARIO 1

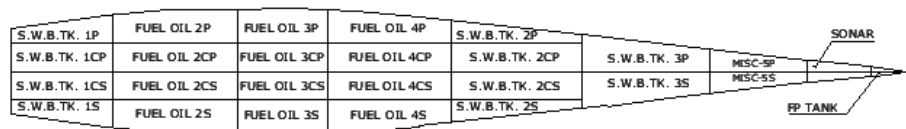
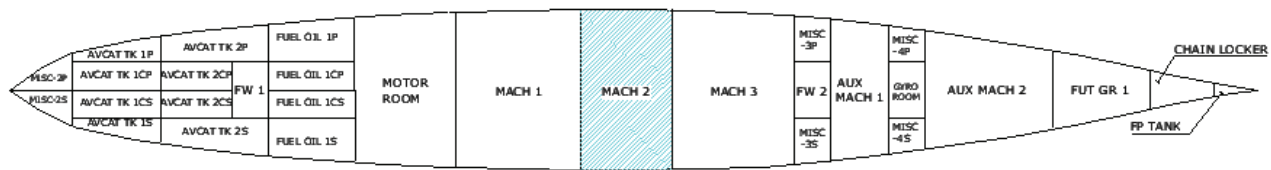
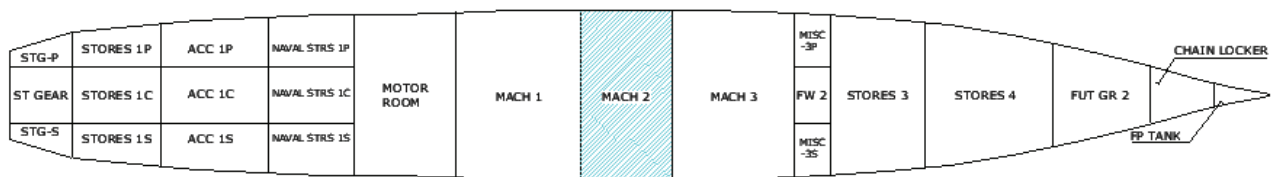
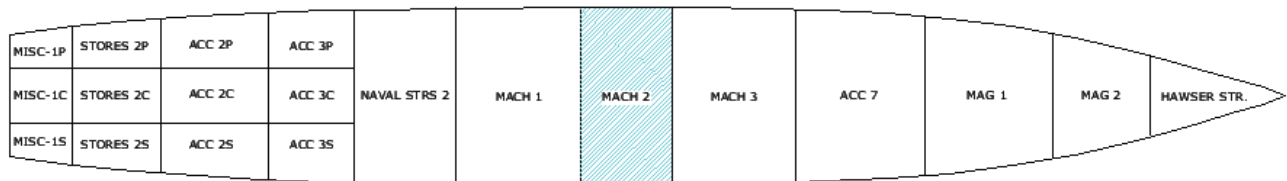
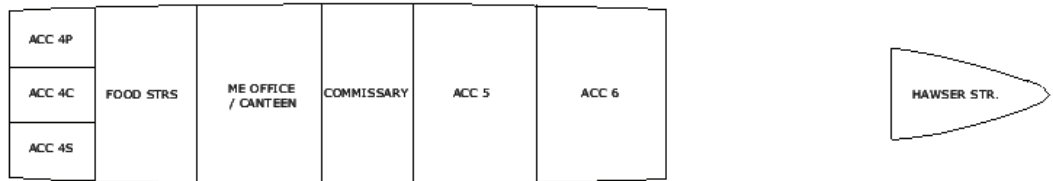
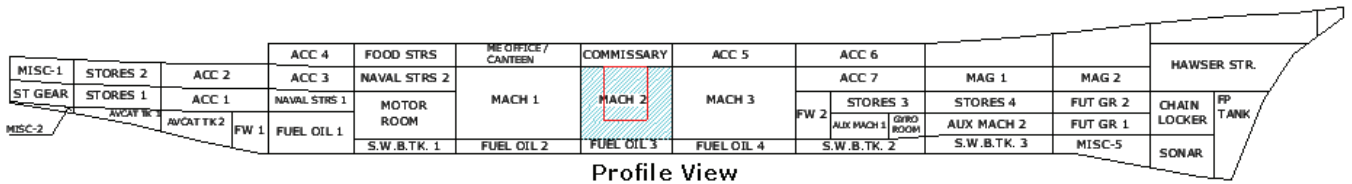
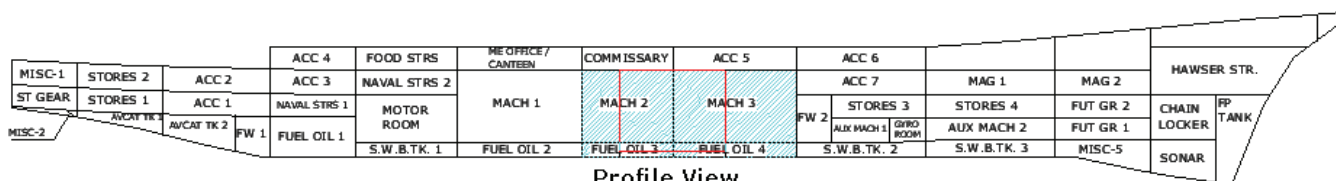
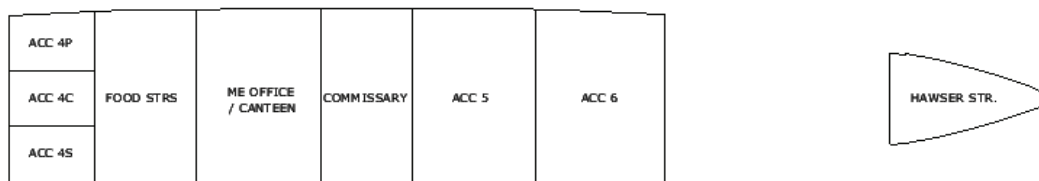


Figure 9: Damage scenario 1

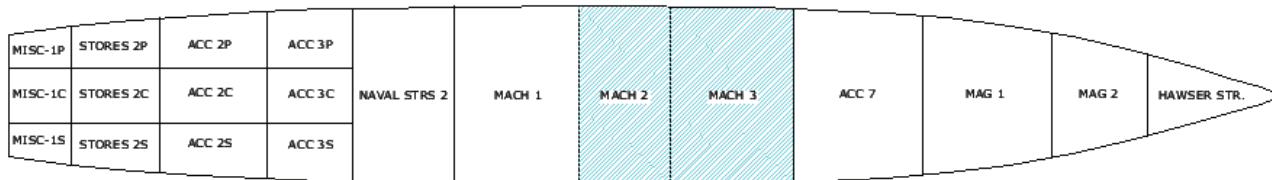
DAMAGE SCENARIO 2



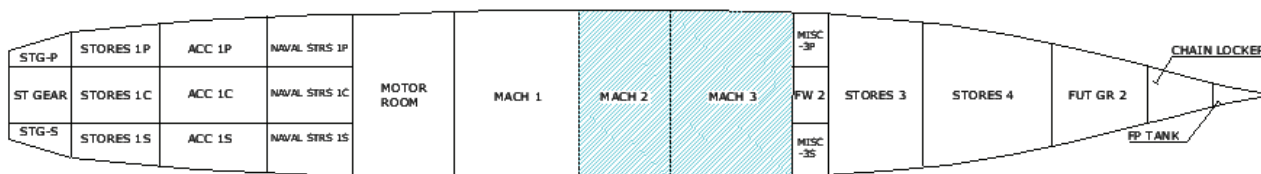
Profile View



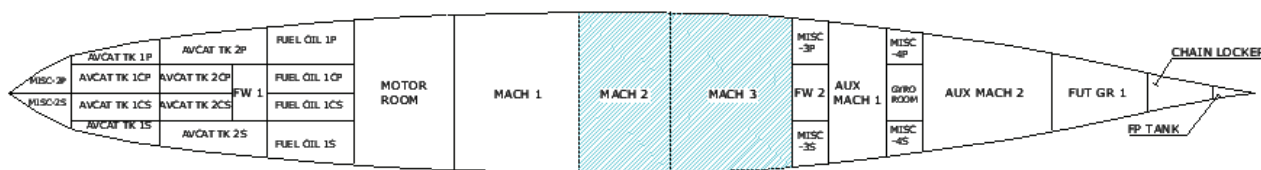
01 Level Plan View at 12.497 metre



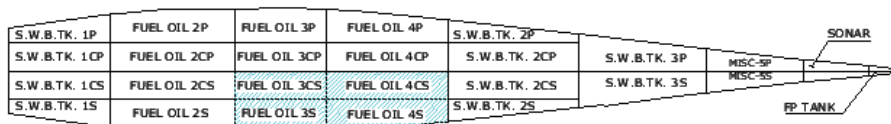
Main Deck Plan View at 9.906 metre



1st Platform Plan View at 7.112 metre



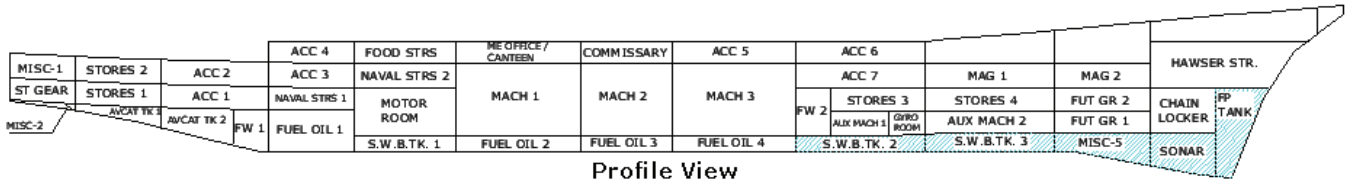
2nd Platform Plan View at 4.496 metre



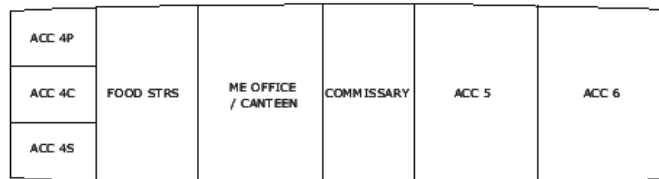
Inner-BTM Plan View at 1.662 metre

Figure 10: Damage scenario 2

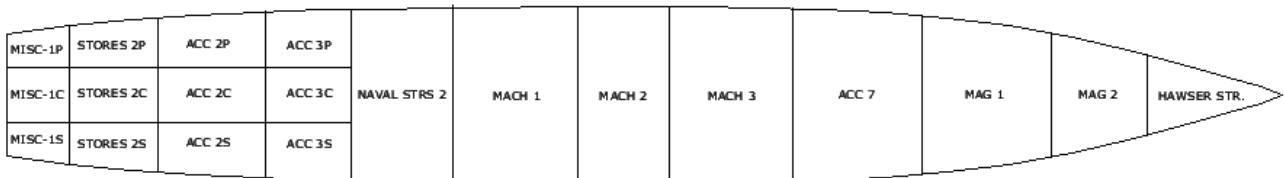
DAMAGE SCENARIO 4



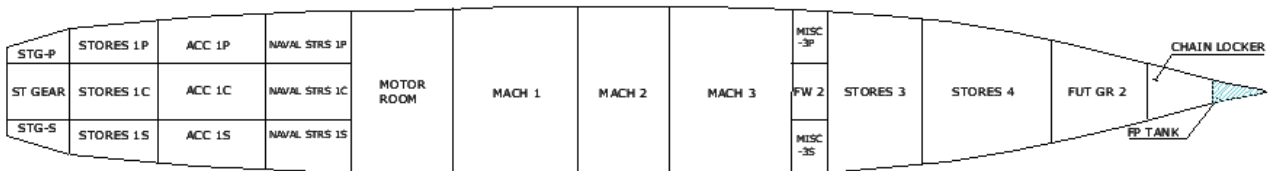
Profile View



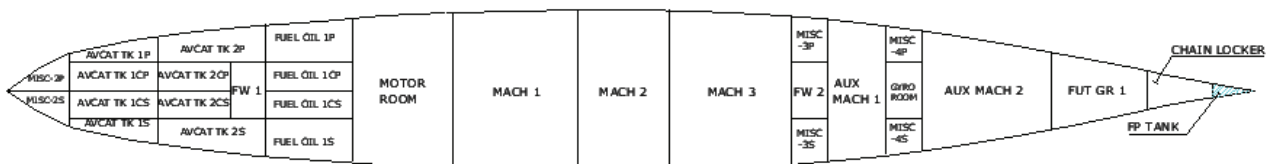
01 Level Plan View at 12.497 metre



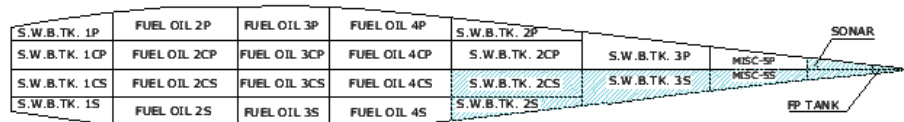
Main Deck Plan View at 9.906 metre



1st Platform Plan View at 7.112 metre



2nd Platform Plan View at 4.496 metre



Inner-BTM Plan View at 1.662 metre

Figure 12: Damage scenario 4

THE RESULTS AND DISCUSSIONS

The computation procedure of this study using UNEW Hydro Programme is provided in Figure 13. In this study 2D linear suite which consists of HULSUR2D for hull form

modeling, MOTION2D for hydrodynamic coefficient and ship motion calculations and WAVED2D for global load calculations was used. The simulations were carried out with 19 cases in intact and four damage conditions (see Table 5).

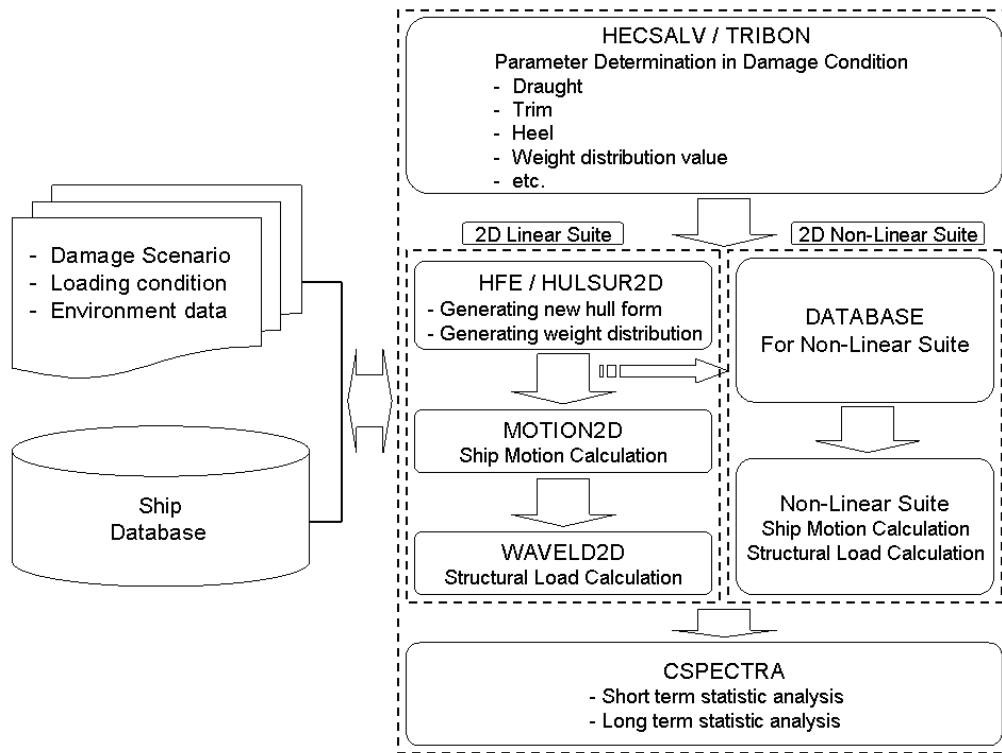


Figure 13: Computation procedure of UNEW Hydro Programme

Weight distribution and global static loads

This section provides weight distribution and hydrostatic information for predicting the global static loads and hydrodynamic loadings on the sample vessel 'H5415' using UNEW hydro programme developed during this research. The data in this part serves as the basis for all the numerical calculations so that the comparison would be made on the same ground.

Figure 14 shows H5415 vessel modelled for initial hydrostatic information of UNEW Hydro programme using HECSALV. Weight distribution in full load departure condition of intact H5415 vessel is shown in Figure 15. The weight distribution of H5415 in full loading departure is used. So far the fuel oil to reflect burn off prior to the incident was not considered in modeling and computations. Tables 6 to 9 describe flooding summaries on different damage scenarios. Table 10 shows information of draught and hydrostatics at equilibrium in intact and damaged conditions. The static vertical shear force distribution and vertical bending moment distribution are presented in Figures 16 and 17.

Stillwater shear forces and bending moments are calculated by results of the difference between buoyancy and mass intensity

along the ship length. In sign convention of vertical shear force and bending moment upward force on the cut of aft portion and sagging are positive. Maximum bending moment in the intact condition is hogging and occurs amidships while two peaks of vertical shear force have opposite sign and take place at about one quarter ship length from either end. When the damaged ship is heeled, the vertical shear force and bending moments measured perpendicular to the still water surface. The results of maximum bending moments and vertical shear forces in damage scenarios 3 and 4 show same trends. The values in damage scenarios 3 and 4 are greater than those of the intact ship. On the other hand, four peak points of vertical shear force and three peak points of vertical bending moment are shown in damage conditions amidships (damage scenarios 1 and 2). The second and third peak of vertical shear forces occur at the ends of the damaged compartment with upward shear at the aft end and downward shear at the fore end because buoyancy is larger than weight at stern and flooding water is in the damaged compartment. In addition the magnitude of the maximum shear force in damage scenario 2 is larger than that in the intact condition and other damaged conditions. And also the ship in damage condition 2 suffers from sagging bending moment amidships and hogging bending moment in the rest of the ship.

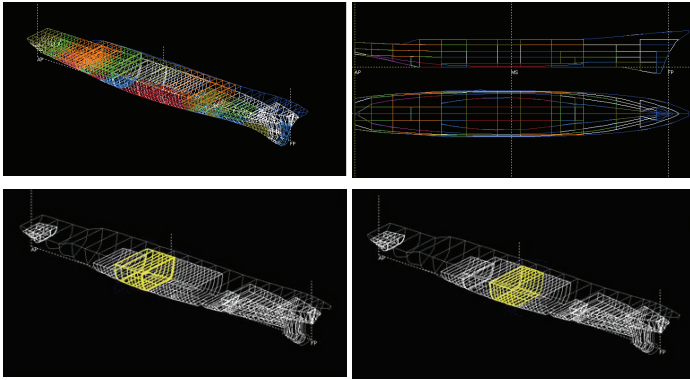


Figure 14: H5415 vessel modelled for initial hydrostatic information of UNEW Hydro programme using HECSALV

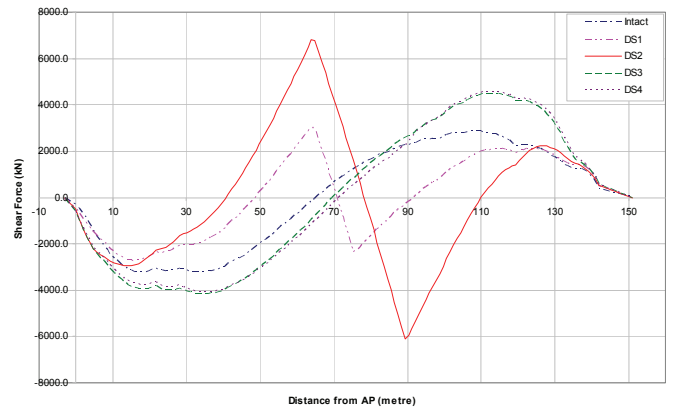


Figure 16: Distribution of static vertical shear force on H5415

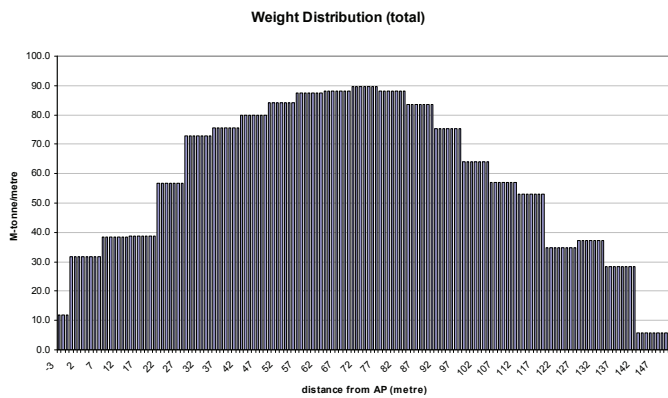


Figure 15: Weight distribution of intact 'H5415' vessel

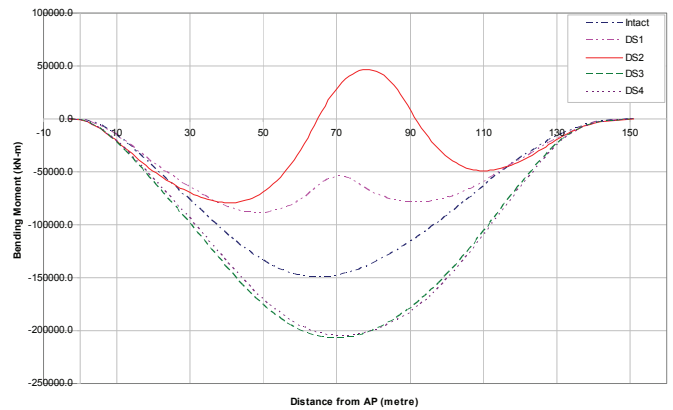


Figure 17: Distribution of static vertical bending moment on H5415

Table 5: Intact and damage conditions investigated

Intact and Damaged Conditions Investigated								
Case	Condition	Displ. (tonne)	Mean draught (m)	Trim (m)	Heel (deg.)	Heading angle (deg.)	Model test	Computation
1	Intact	9032.2400	6.3094	0.0000	0.0000	180.0000	OK	OK
2	Intact	9032.2400	6.3094	0.0000	0.0000	45.0000	OK	OK
3	Intact	9032.2400	6.3094	0.0000	0.0000	90.0000	OK	OK
4	Damage Scenario 1	9905.0000	6.6830	0.2260F	0.0000	180.0000	N/A	OK
5	Damage Scenario 1	9905.0000	6.6830	0.2260F	0.0000	45.0000	N/A	OK
6	Damage Scenario 1	9905.0000	6.6830	0.2260F	0.0000	90.0000	N/A	OK
7	Damage Scenario 2	11450.0000	7.4175	1.4330F	1.100S	180.0000	OK	OK
8	Damage Scenario 2	11450.0000	7.4175	1.4330F	1.100S	45.0000	OK	OK
9	Damage Scenario 2	11450.0000	7.4175	1.4330F	1.100S	90.0000	OK	OK
10	Damage Scenario 2	11450.0000	7.4175	1.4330F	1.100S	270.0000	OK	OK
11	Damage Scenario 2	11450.0000	7.4175	1.4330F	1.100S	315.0000	OK	OK
12	Damage Scenario 3	9331.0000	6.4485	0.8370F	0.0000	180.0000	OK	OK
13	Damage Scenario 3	9331.0000	6.4485	0.8370F	0.0000	45.0000	OK	OK
14	Damage Scenario 3	9331.0000	6.4485	0.8370F	0.0000	90.0000	OK	OK
15	Damage Scenario 4	9439.0000	6.5055	1.0320F	0.400S	180.0000	N/A	OK
16	Damage Scenario 4	9439.0000	6.5055	1.0320F	0.400S	45.0000	N/A	OK
17	Damage Scenario 4	9439.0000	6.5055	1.0320F	0.400S	90.0000	N/A	OK
18	Damage Scenario 4	9439.0000	6.5055	1.0320F	0.400S	270.0000	N/A	OK
19	Damage Scenario 4	9439.0000	6.5055	1.0320F	0.400S	315.0000	N/A	OK

Table 6: Flooding summary on damage scenario 1

Compartment	Seawater MT	Oil MT	Perm.	For equilibrium at 0.0 deg.				TCG m-CL	FSc m	Sounding m	Specified % Full	Pressure barG
				Density MT/m3	VCG m	LCG m-AP						
MACH-2	797	----	0.850	1.0250	4.264	69.793F	0.000S	0.001	----	58.000	----	
Totals	797	0			4.264	69.793F	0.000S	0.001				

Table 7: Flooding summary on damage scenario 2

Compartment	Seawater MT	Oil MT	Perm.	For equilibrium at 1.1 deg. S				TCG m-CL	FSc m	Sounding m	Specified % Full	Pressure barG
				Density MT/m3	VCG m	LCG m-AP						
MACH-2	921	----	0.850	1.0250	4.635	69.809F	0.117S	0.001	----	67.000	----	
MACH-3	1,227	----	0.850	1.0250	4.741	81.929F	0.116S	0.001	----	68.000	----	
FO-3CS	52	----	0.990	1.0250	0.883	69.793F	1.534S	0.000	----	100.000	----	
FO-3S	37	----	0.990	1.0250	1.141	69.740F	4.671S	0.000	----	100.000	----	
FO-4CS	67	----	0.990	1.0250	0.910	81.895F	1.511S	0.000	----	100.000	----	
FO-4S	37	----	0.990	1.0250	1.187	81.221F	4.407S	0.000	----	100.000	----	
Totals	2,342	0			4.390	76.686F	0.329S	0.001				

Table 8: Flooding summary on damage scenario 3

Compartment	Seawater MT	Oil MT	Perm.	For equilibrium at 0.0 deg.				TCG m-CL	FSc m	Sounding m	Specified % Full	Pressure barG
				Density MT/m3	VCG m	LCG m-AP						
MISC-5P	25	----	0.850	1.0250	1.099	123.590F	0.636P	0.000	----	100.000	----	
MISC-5S	25	----	0.850	1.0250	1.099	123.590F	0.636S	0.000	----	100.000	----	
SONAR	79	----	0.850	1.0250	-0.437	133.522F	0.000S	0.000	----	100.000	----	
FOREPEAK-TK	95	----	0.990	1.0250	1.544	138.469F	0.000S	0.000	----	98.000	----	
Totals	223	0			0.745	133.424F	0.000P	0.000				

Table 9: Flooding summary on damage scenario 4

Compartment	Seawater MT	Oil MT	Perm.	For equilibrium at 0.4 deg. S				TCG m-CL	FSc m	Sounding m	Specified % Full	Pressure barG
				Density MT/m3	VCG m	LCG m-AP						
SW-2CS	62	----	0.990	1.0250	1.017	96.161F	1.403S	0.000	----	100.000	----	
SW-2S	12	----	0.990	1.0250	1.359	94.111F	3.834S	0.000	----	100.000	----	
SW-3S	58	----	0.990	1.0250	1.337	110.293F	1.217S	0.000	----	100.000	----	
MISC-5S	25	----	0.850	1.0250	1.099	123.590F	0.636S	0.000	----	100.000	----	
SONAR	79	----	0.850	1.0250	-0.437	133.522F	0.000S	0.000	----	100.000	----	
FOREPEAK-TK	97	----	0.990	1.0250	1.653	138.478F	0.000S	0.000	----	100.000	----	
Totals	332	0			0.932	121.805F	0.659S	0.000				

Table 10: Draught and hydrostatics at equilibrium

	Intact condition	Damage scenario 1	Damage scenario 2	Damage scenario 3	Damage scenario 4	Unit
Draft at AP	6.310	6.570	6.701	6.030	5.990	metres
Draft at FP	6.310	6.796	8.134	6.867	7.021	metres
Total Weight	9032.240	9905.000	11450.000	9331.000	9439.000	MT
VCG	6.283	6.120	5.895	6.150	6.095	metres
LCG	70.078F	70.055F	71.429F	71.590F	71.895F	m-AP
TCG	0.000S	0.000S	0.067S	0.000P	0.023S	m-CL
Buoyancy	9032.240	9905.000	11450.000	9331.000	9439.000	MT
KB	3.743	3.963	4.386	3.809	3.842	metres
LCB	70.117F	70.057F	71.449F	71.604F	71.912F	m-AP
TCB	0.000S	0.000S	0.098S	0.000	0.040S	m-CL
KMt	9.470	9.431	9.409	9.434	9.426	metres
FSc	0.061	0.596	1.164	0.060	0.059	metres
GMt	3.126	2.675	2.314	3.181	3.229	metres

Predictions of Global Dynamic Wave-Induced Loads Using 2D Linear Method

The global dynamic wave induced loads acting on HULL5415 in various design conditions have been calculated using a 2D linear method, and are compared to examine the damage effects on the sample vessel 'H5415' along the vessel length from Aft Perpendicular to Fore Perpendicular. Figures 18 to 21 show the correlations of the computation results of vertical bending moments, horizontal bending moments and torsion moments in intact and damage conditions. Here damage scenario 1 (cases 4 and 5) and damage scenario 2 (cases 7, 8 and 11) stand for one and two compartment flooding damage conditions amidships respectively. Damage scenario 3 (cases 12 and 13) and damage scenario 4 (cases 15, 16 and 19) are related to the compartment flooding damages at fore body in the ship.

Figure 18 shows that in head waves the maximum vertical bending moment RAO in cases 4 and 7 (damage scenarios 1 & 2) is larger than that of intact condition, while the results in cases 12 and 15 (damage scenarios 3 & 4) show opposite. In addition case 7 (damage scenario 2) is the worst condition because its maximum vertical bending moment RAO is increased the most, and occurs amidships, where damage is imposed. This is probably due to the fact that the draught is increased the most (by 1.1 meters) in damage scenario 2.

Comparison of vertical bending moments at stern quartering waves is shown in Figure 19. This figure shows that the vertical bending moment in intact condition is larger than those in damaged conditions. In Figure 20 it can be seen that the horizontal bending moment RAOs in damage scenario 2 (cases 8 & 11) are the largest, and followed by damage scenario 1 (case 5), intact condition (case 2) and others. Figure 21 shows comparison of torsion moment at stern quartering waves. The torsional moment in the intact ship is the least amongst all the conditions, while damage scenario 2 (cases 8 & 11) has the largest torsional moment. Bearing in mind that damage scenario 2 has the largest opening, its torsional strength could be a concern.

Comparison of numerical predictions and measurements of global dynamic wave loads

Comparison in intact condition

The global dynamic wave induced loads calculated using 2D linear method and measurements of intact H5415 vessel in three different wave angles are presented in Figures 22 to 24. The correlation between the predicted and measured values shows that the agreement in large waves is slightly better than those in small waves. But the differences in the experiment values according to wave amplitudes are small. The correlation between the computations and measurements of global dynamic wave induced load response amplitudes of the intact ship is reasonable for head and stern quartering waves while the differences of the results in beam waves are significant. Nevertheless the magnitude of loads in beam waves is usually very small, so the large difference in numerical prediction would not cause much concern in the strength assessment of hull girders. Overall the

2D linear strip method presents acceptable agreements with the measurements. This will be further examined by calculating the model uncertainty of the 2D linear method.

Comparison in damage scenario 2

The global dynamic wave induced loads calculated using 2D linear method and measurements of DS2 H5415 vessel in five different wave angles are presented in the following figures.

- Figures 25 to 28 for DS2 ship in head waves.
- Figures 29 to 32 for DS2 ship in stern quartering waves ($\beta=45$).
- Figures 33 to 36 for DS2 ship in beam waves ($\beta=90$).

In the experiments the global dynamic wave induced loads with two different wave amplitudes were investigated. The correlation between the predicted and measured values shows that the measurements under large waves and small waves are not significantly different.

In head and stern quartering waves, the differences between the computations and measurements of global dynamic wave induced load response amplitudes of DS2 ship with different wave amplitudes are reasonable. The 2D linear method presents acceptable agreements with the measurements. However the differences between the predictions and measurements of dynamic torsion moments are significant. And these phenomena could be caused by the effects of sloshing within the damaged compartments, which could reduce the global dynamic wave load components.

The measured and predicted dynamic wave induced loads in beam waves are in good agreements for vertical shear forces and vertical bending moments while there are significant differences in the results of horizontal dynamic wave induced load components. The possible reasons for this difference are the sloshing effects within the damaged compartment. In addition the drift of model may also be attributed to this difference.

Prediction of Extreme Design Loads

The distributions of the most probable extreme amplitudes of global dynamic wave induced vertical and horizontal bending moments on the sample vessel 'H5415' in intact and different damaged conditions were calculated using dynamic wave induced vertical and horizontal bending moment response amplitudes obtained from numerical calculations in stochastic analysis. The modified Pierson-Moskowitz (ISSC) spectrum with two parameters was used in the spectral analysis. Intact vessels should be capable of withstanding design defined sea states. In this study a marginally operational condition is employed for the intact ship. The ISSC committee mentioned that the ship hull girder after damaged can be able to survive for four days in mean sea conditions (ISSC, 2006). In numerical predictions, a 20 years wave condition at a sea state 5 was used for the intact condition, while a sea state of 3 for 96 hours was used for damaged condition. Table 11 summarises the calculated values of the stillwater bending moment, extreme dynamic wave induced bending and torsion moments on intact H5415 in head and stern quartering waves.

Similarly the calculated values of the stillwater bending moment, extreme dynamic wave induced bending and torsion moments for damaged H5415 model are summarised in Tables 12a and 12b. One and two compartment damaged conditions amidships are the worst conditions for the most probable extreme amplitudes of dynamic wave induced vertical and horizontal bending moments in head and stern quartering waves. It is shown that the differences of torsion moments between case 8 (heading 45) and case 11 (heading 315) are quite large as around 25% value differences amidships. Both Cases 8 and 11 are for damage scenario 2. This means that the effects caused by heading are important for torsion moments in stern quartering waves. The most extreme loads for damage scenarios 3 and 4 (Cases 13, 16 and 19) are less than those for damage scenarios 1 and 2 (cases 5, 8 and 11).

The maximum values of the most probable extreme amplitudes of dynamic wave induced loads in damaged conditions are much less than those in intact condition, because the most probable extreme design load in intact condition is

based on long term prediction with a duration of 20 years (sea state 5), while the most probable extreme design load for damaged conditions is based on short term prediction (sea state 3 for 96 hours). However the loads in damage scenarios 1 and 2 are important to assess the residual strength of the damaged ship due to her loss of the most main structural members amidships.

The distribution of the total loads including stillwater bending moment and wave-induced bending moment over the ship length has been plotted in Figures 37 to 40 to show how each damage changes the distribution of total loads and each load component. These curves could be used to identify the critical cross sections, which need strength assessment after damage, apart from the damaged cross sections. It is interesting to note that the total vertical bending moment over the whole length of the ship in intact condition is greater than that in damage scenarios 1 and 2. However in damage scenarios 3 and 4 in some cross sections the total vertical bending moment in the damaged condition is slightly greater than that in intact condition although it is opposite in majority of the areas.

Head waves

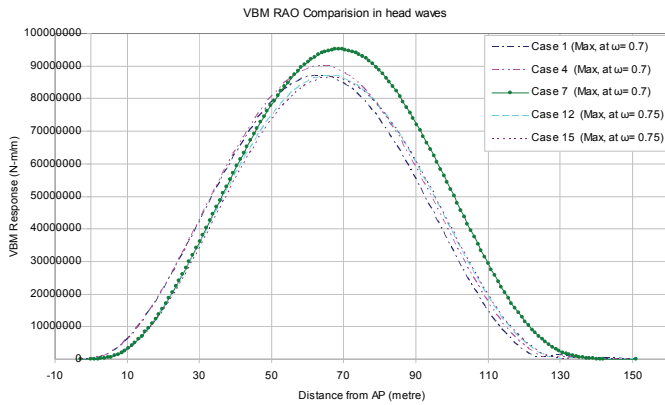


Figure 18: Vertical bending moment RAO comparison at head waves

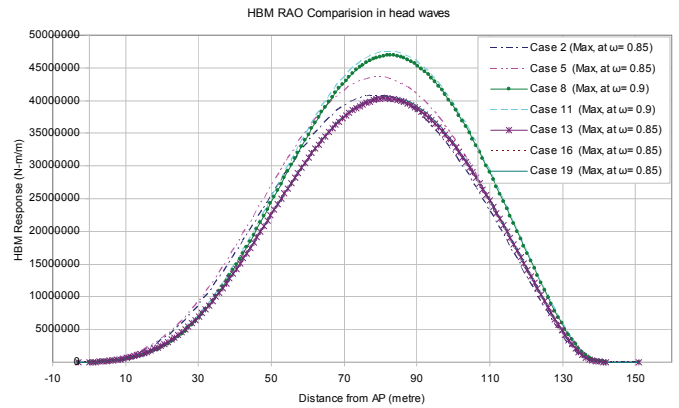


Figure 20: Horizontal bending moment RAO comparison at stern quartering waves

Stern quartering waves

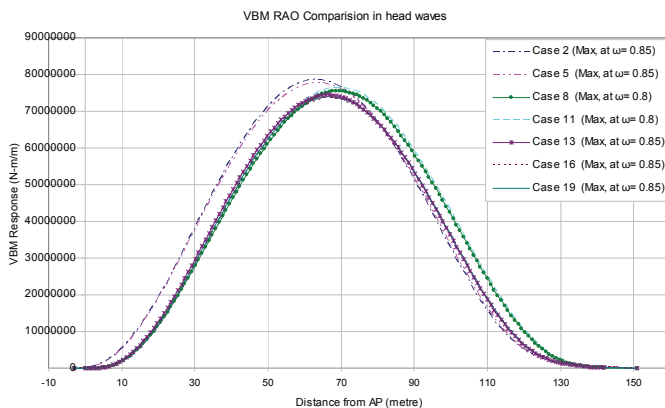


Figure 19: Vertical bending moment RAO comparison at stern quartering waves

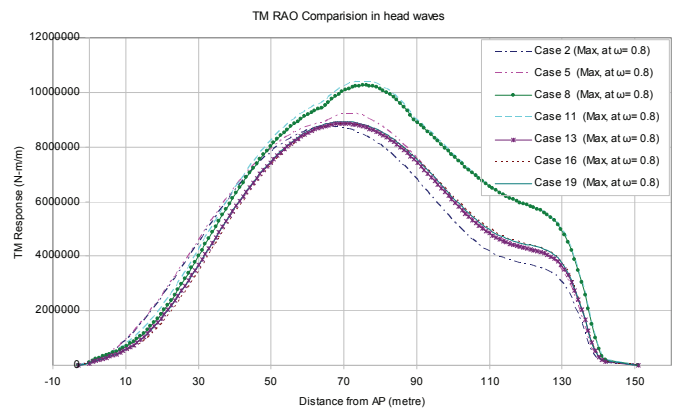


Figure 21: Torsion moment RAO comparison at stern quartering waves

Head waves

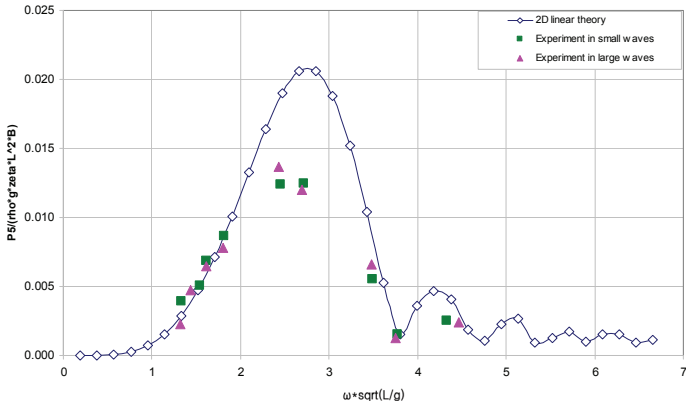


Figure 22: Dynamic vertical bending moment force RAO of intact H5415 at head waves

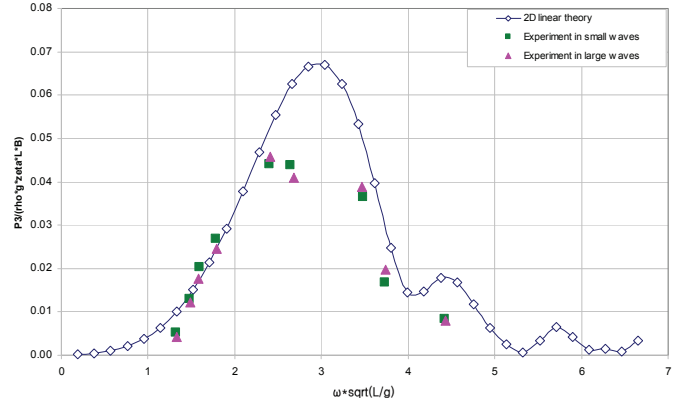


Figure 25: Dynamic vertical shear force RAO of DS2 H5415 at head waves

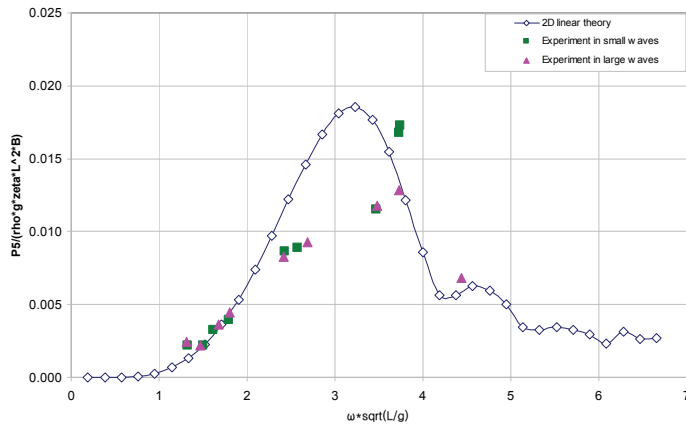


Figure 23: Dynamic vertical bending moment RAO of intact H5415 at stern quartering waves

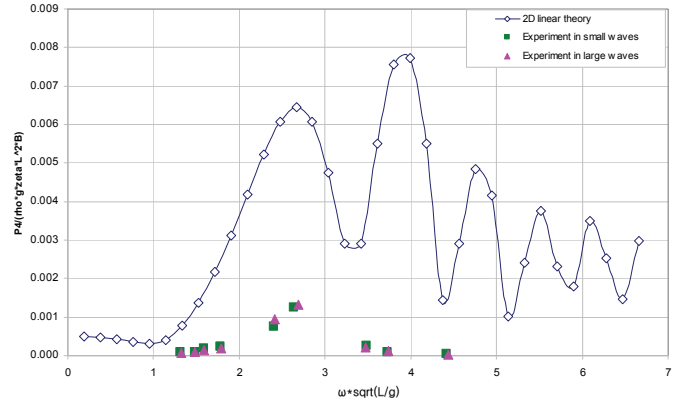


Figure 26: Dynamic torsion moment RAO of DS2 H5415 at head waves

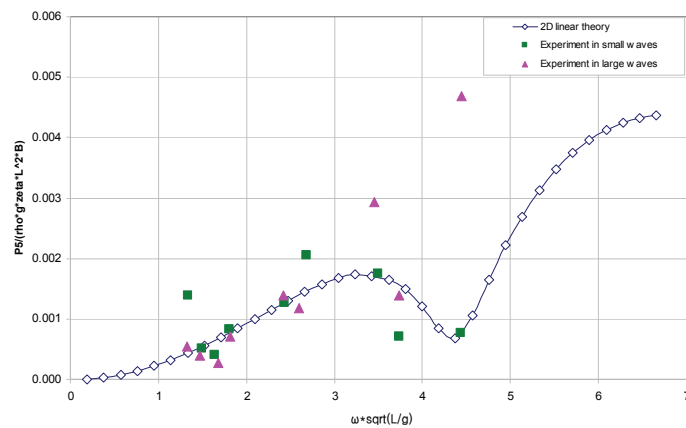


Figure 24: Dynamic vertical bending moment RAO of intact H5415 at beam waves

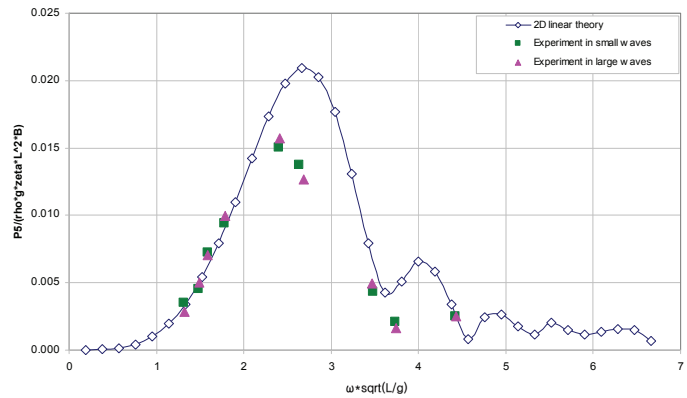


Figure 27: Dynamic vertical bending moment RAO of DS2 H5415 at head waves

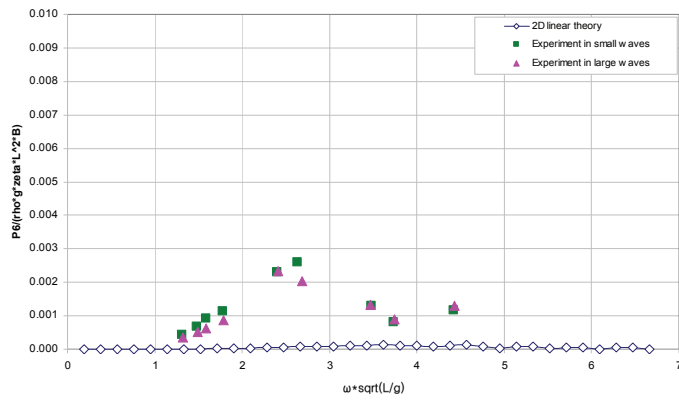


Figure 28: Dynamic horizontal bending moment RAO of DS2 H5415 at head waves

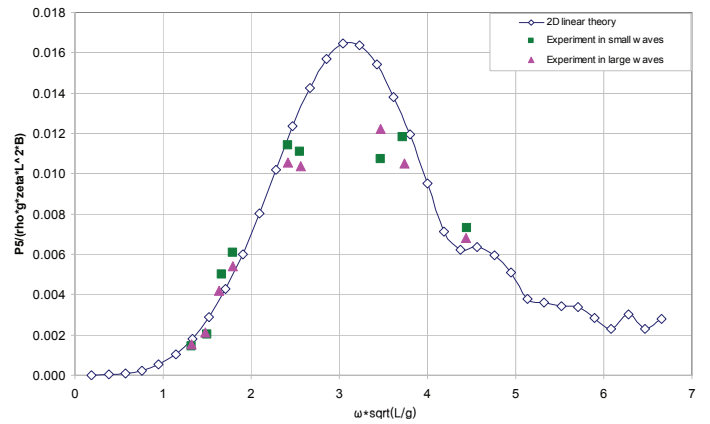


Figure 31: Dynamic vertical bending moment RAO of DS2 H5415 at stern quartering waves (heading 45)

Stern quartering waves (heading 45)

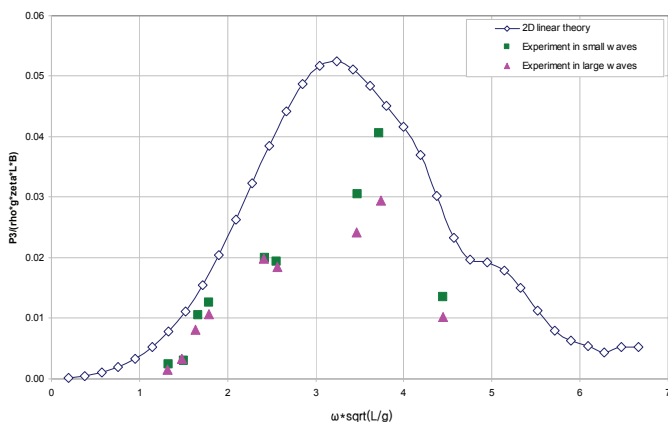


Figure 29: Dynamic vertical shear force RAO of DS2 H5415 at stern quartering waves (heading 45)

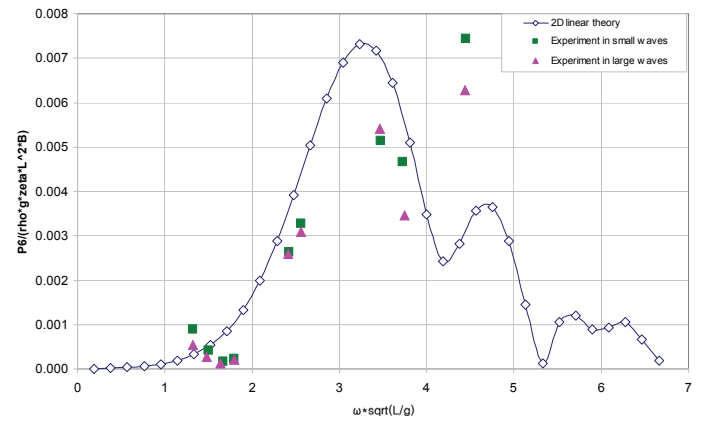


Figure 32: Dynamic horizontal bending moment RAO of DS2 H5415 at stern quartering waves (heading 45)

Beam waves (heading 90)

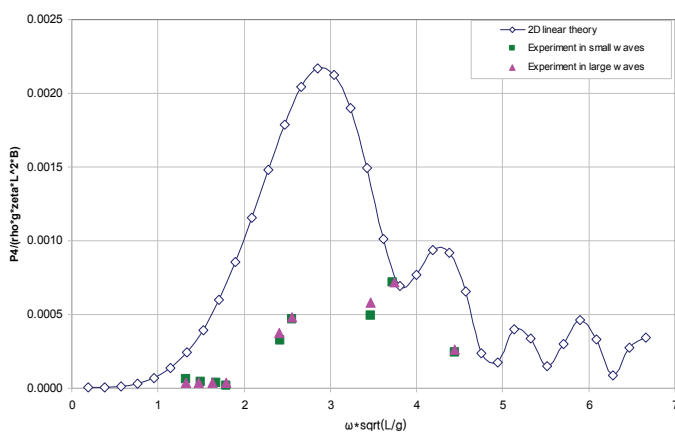


Figure 30: Dynamic torsion RAO of DS2 H5415 at stern quartering waves (heading 45)

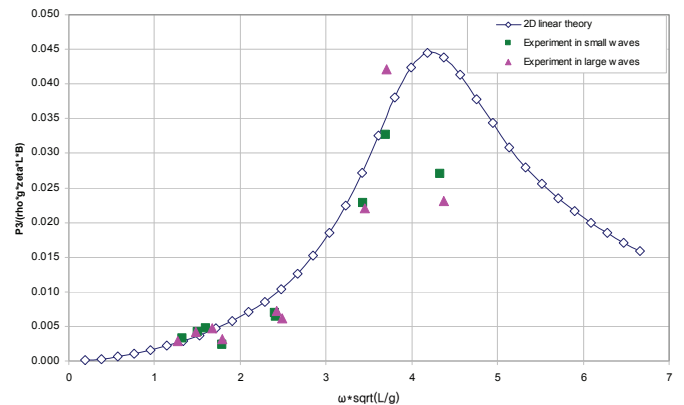


Figure 33: Dynamic vertical shear force RAO of DS2 H5415 at beam waves (heading 90)

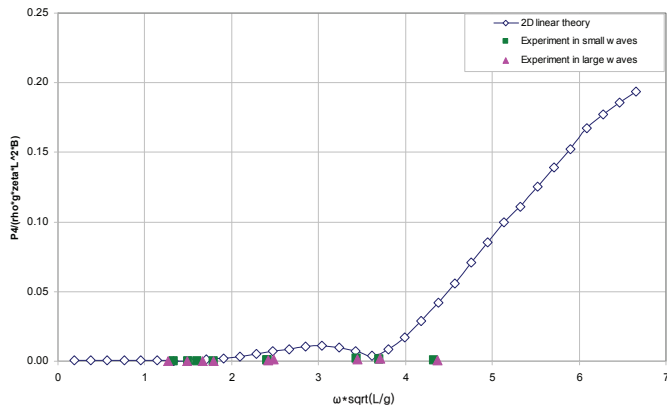


Figure 34: Dynamic torsion moment RAO of DS2 H5415 at beam waves (heading 90)

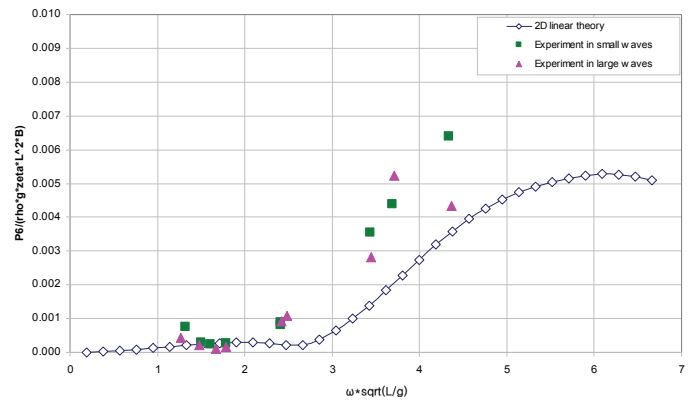


Figure 36: Dynamic horizontal bending moment RAO of DS2 H5415 at beam waves (heading 90)

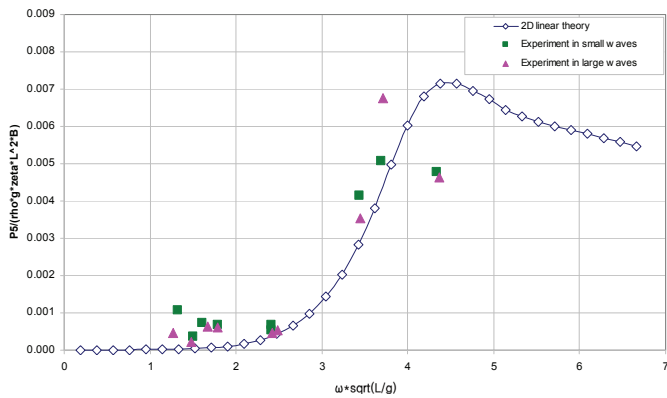


Figure 35: Dynamic vertical bending moment RAO of DS2 H5415 at beam waves (heading 90)

Table 11: Bending and torsion moments (kN-m) for intact H5415 model (at midship)

SWBM	in head waves		in stern quartering waves		
	WVBM	WVBM	WHBM	WTM	WTM
	case1	case2	case2	case2	case2
147610	335580	287740	138370	32860	

Table 12a: Bending moments (kN-m) for damaged H5415 ship (at midship)

SWBM in DS1	SWBM in DS2	SWBM in DS3	SWBM in DS4	in head waves				in stern quartering waves				
				WVBM	WVBM	WVBM	WVBM	WVBM	WVBM	WVBM	WVBM	WVBM
				case4	case7	case12	case15	case5	case8	case11	case13	case16
54588	-30934	207161	205003	59822	61585	59809	59379	62986	63610	64275	61240	60734

where, case 5: damage scenario 1, cases 8 & 11: damage scenario 2, case 13: damage scenario 3 and cases 16 & 19: damage scenario 4

Table 12b: Bending and torsion moments (kN-m) for damaged H5415 ship (at midship)

in stern quartering waves												
WVBM	WHBM	WHBM	WHBM	WHBM	WHBM	WHBM	WTM	WTM	WTM	WTM	WTM	WTM
case19	case5	case8	case11	case13	case16	case19	case5	case8	case11	case13	case16	case19
61066	33740	35400	35950	31019	31097	31313	7086	7668	7785	6955	6986	7016

where, case 5: damage scenario 1, cases 8 & 11: damage scenario 2, case 13: damage scenario 3 and cases 16 & 19: damage scenario 4

In head waves

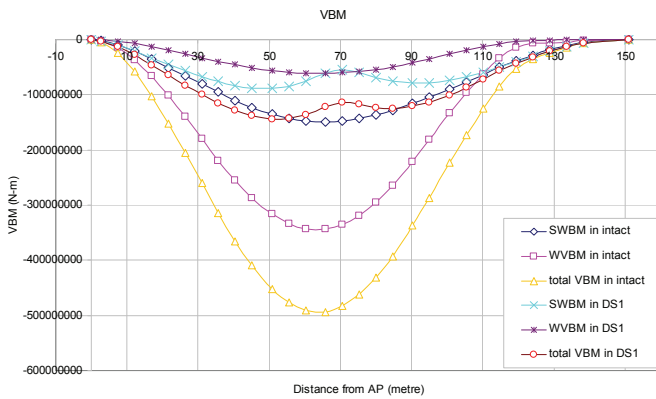


Figure 37: Comparison of the total loads in intact and damage scenario 1

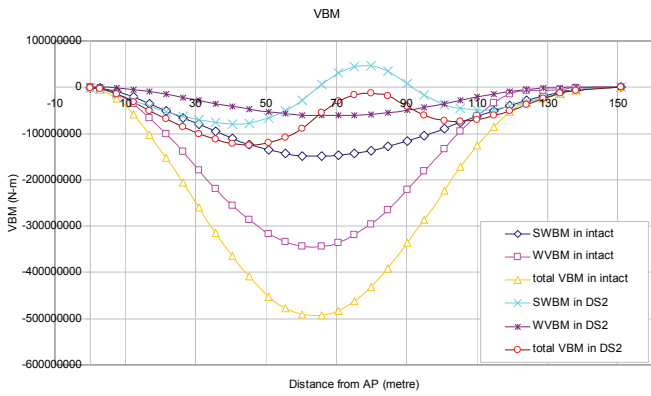


Figure 38: Comparison of the total loads in intact and damage scenario 2

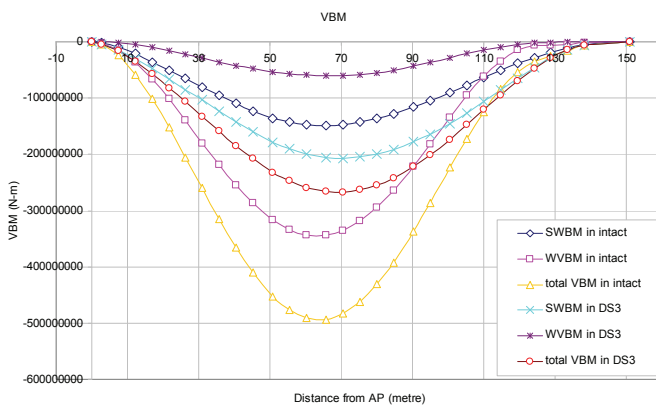


Figure 39: Comparison of the total loads in intact and damage scenario 3

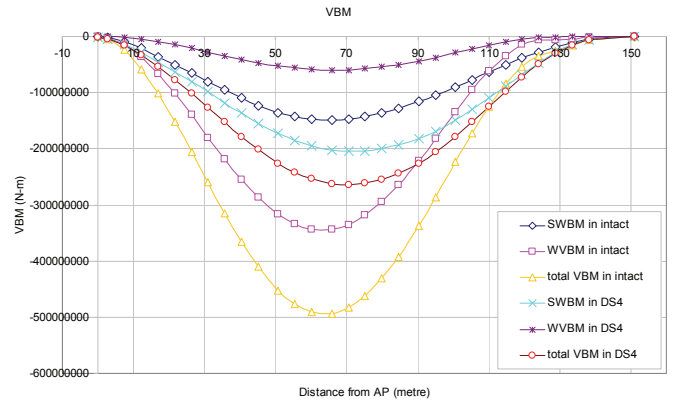


Figure 40: Comparison of the total loads in intact and damage scenario 4

CONCLUSIONS

The hydrodynamic loads in regular waves have been calculated by a 2D linear method, and extreme design loads have been predicted by spectral analysis. Experimental tests on a ship model with a scale of 1/100 have also been carried out to predict the hydrodynamic loads in regular waves. The results of the theoretical method and experimental tests are compared to validate the theoretical method.

It is found that in head waves a large opening, such as damage scenario 2, can dramatically increase wave-induced vertical bending moment. This is mainly attributed to the large increase of draught. But in damage scenarios 3 and 4 the vertical bending moment is slightly reduced.

In stern quartering waves the vertical bending moment in intact condition is larger than those in damaged conditions. However the horizontal bending moment RAOs in damage scenario 2 are the largest, and followed by damage scenario 1, intact condition and others. The torsional moment in the intact ship is the least amongst all the conditions, while damage scenario 2 has the largest torsional moment. Bearing in mind that damage scenario 2 has the largest opening, its torsional strength could be a concern.

In beam waves the magnitude of wave-induced loads is much smaller than those in other headings, so this would not cause any concern from structural strength point of view.

The comparison of theoretical results with experimental results has revealed that:

- a) In intact condition, the agreement in large waves is slightly better than those in small waves. But the differences in the experimental results according to wave amplitudes are small. The computations and measurements of global dynamic wave induced load response amplitudes are in good agreement in head and stern quartering waves while the differences of the results in beam waves are significant. Nevertheless the magnitude of loads in beam waves is usually very small, so the large difference in numerical prediction would not

cause much concern in the strength assessment of hull girders. Overall the 2D linear strip method presents acceptable agreements with the measurements.

b) In damage scenario 2 the 2D linear method has acceptable agreements with the measurements for vertical and horizontal bending moments. However the differences between the predictions and measurements of dynamic torsion moments are significant. And these phenomena could be caused by the effects of sloshing within the damaged compartments, which could reduce the global dynamic wave load components. The measured and predicted dynamic wave induced loads in beam waves are in good agreements for vertical shear forces and vertical bending moments while there are significant differences in the results of horizontal dynamic wave induced load components. The possible reasons for this difference are the sloshing effects within the damaged compartment. In addition the drift of model may also be attributed to this difference.

c) In damage scenario 3, the measurements in large waves produce slightly better agreements with numerical results than those in small waves. In head and stern quartering waves, the correlation between the computations and measurements of dynamic load response amplitudes for DS3 ship is satisfactory. The wave induced loads in beam waves are not important because they are small values compared to the other load components.

d) It is observed that the accuracy for vertical bending moment is generally better than that for horizontal bending moment, and the COV of horizontal bending moment is almost as twice as that of vertical bending moment. It may be logical to consider model uncertainties for vertical bending moment and horizontal bending moment separately in reliability analysis. However this could be the further research topic. The accuracies at different floating conditions (intact, DS2 and DS3) are slightly different, but are comparable.

The extreme design wave-induced loads have been calculated by short term prediction. For the loads in intact condition, the extreme design wave-induced loads with duration of 20 years is used, while for loads in damaged conditions short term prediction is used. The maximum values of the most probable extreme amplitudes of dynamic wave induced loads in damaged conditions are much less than those in intact condition, because the most probable extreme design load in intact condition is based on the prediction with 20 years exposure time, while the most probable extreme design load for damaged conditions is based on short term prediction (sea state 3 for 96 hours).

It is noticed that when a ship is damaged, the critical cross sections, whose strength needs to be assessed, are not necessarily limited to the damaged cross sections only. Although some cross sections are not structurally damaged, the total loads acting on these cross sections after damage (in other locations) may be increased compared to the original design load in intact

condition. In this case the strength of these cross sections also needs to be assessed.

ACKNOWLEDGEMENT

The authors wish to acknowledge Dr. Paul Hess for his enthusiastic and enormous effort to secure the funding and then actively collaborate with us in this project. Our gratitude goes to ONR for sponsoring this research. The contributions of Prof. Mehmet Atlar and Prof. Martin Downie of Newcastle University are also acknowledged.

It is noted that all research works in this paper were carried out during Dr. Yongwon Lee's PhD course at Newcastle University. He is currently employed by Lloyd's Register.

REFERENCES

- Bhattacharyya, R. (1978). *"Dynamics of Marine Vehicles"*, Ocean Engineering Series, J. Wiley, New York.
- Brebbia, C. A. and Walker, S. (1979). *"Dynamic analysis of offshore structures"*, Butterworth & Co. ISBN: 0-408-00393-6.
- Chan, H. S. (1992). "Dynamic structural responses of a mono-hull vessel to regular waves", *International Shipbuilding Progress*, Vol. 39, pp.287-315.
- Chan, H.S., Incecik, A. and Atlar, M. (2001). "Structural Integrity of a Damaged Ro-Ro Vessel" *Proceedings of the second international conference on collision and grounding of ships*, Technical University of Denmark, Lybgy, pp. 253-258.
- Chan, H. S., Atlar, M. and Incecik, A. (2002). "Large-amplitude motion responses of a Ro-Ro ship to regular oblique waves in intact and damaged conditions", *J Marine Science and Technology Vol. 7*, pp.91-99.
- Chan, H. S., Atlar, M. and Incecik, A. (2003). "Global wave loads on intact and damaged RO-RO ships in regular oblique waves", *J Marine Structures Vol. 16*, pp.323-344.
- DNV (2000). *"DNV Classification Note 30.5: Environmental Conditions and Environmental Loads"*.
- Faltinsen, O.M. (1990). *"Sea Loads on Ships and Offshore Structures"*, Cambridge Ocean Technology Series, Cambridge University Press. ISBN: 0-521-45870-6.
- Frank, W. (1967). *"Oscillation of Cylinders in or Below the Free Surface of Deep Fluids"*, Hydromechanics Laboratory Research and Development Report.
- Geritsma, J. and Beukelman, W. (1967). "Analysis of the modified strip theory for the calculation of ship motions and wave bending moments", *International shipbuilding progress Vol.14*, no.156.
- ISSC, (1997). "Ultimate Strength". Report of Committee III.1, *International Ships and Offshore Structures Congress*.

- ISSC, (2006). "Naval Ship Design". Report of Committee V.5, *International Ships and Offshore Structures Congress*.
- Jacobs, W.R. (1958). "The analytical calculation of ship bending moments in regular waves". *J Ship Research*, June, pp.20-29.
- Jacobs, W.R., Dalzell, J. and Lalangas, P. (1960). "Guide to computational procedure for analytical evaluation of ship bending-moments in regular waves", *US Navy, Davidson Laboratory*, Report No.791.
- Kim, C. H., Chou, F. S. and Tien, D. (1980) "Motions and hydrodynamic loads of a ship advancing in oblique waves", *Trans SNAME Vol. .88*, pp.225-56.
- Korvin-Kroukovsky, B.V. (1955). "Investigation of ship motions in regular waves", *Transactions SNAME Vol. 63*, pp.386-435.
- Korvin-Kroukovsky, B.V. and Jacobs, W.R (1957). "Pitching and heaving motions of a ship in regular waves". *SNAME Trans Vol. 65*, pp.590-632.
- Korkut, E., Atlar, M. and Incecik, A. (2004), "An experimental study of motion behaviour with an intact and damaged Ro-Ro ship model", *J Ocean Engineering* v.31, pp.483-512.
- Korkut, E., Atlar, M. and Incecik, A. (2005), "An experimental study of global loads acting on an intact and damaged Ro-Ro ship model", *J Ocean Engineering* v.32, pp.1370-1403.
- Lee, C. M. and Curphey, R. M. (1977). "Prediction of motion, stability and wave load of small-waterplane-area, twin-hull ships", *Trans SNAME* v.85, pp. 94-130.
- Lee, Dongkon, Lee, Soon-Sup, Park, Beom-Jin and Kim, Soo-Young. (2005). "A study on the framework for survivability assessment system of damaged ships", *J Ocean Engineering* v.32, pp.1122-1132.
- Lloyd's Register, (2000). *"World Casualty Statistics: annual statistical summary of reported loses and disposals of propelled sea-going merchant ships of not less than 100 GT"*.
- Newman, J. N. (1978). "The theory of ship motions", *Advances in Applied Mechanics* v.18, pp.221-83.
- Ochi, M.K. (1973). "On prediction of extreme values". *J Ship Research*, v.17 n.1, Mar, pp.29-37.
- Ochi, M.K. (1981). "Principles of extreme value statistics and their application". *Extreme Loads Response Symposium (SNAME)*, Arlington, VA, October 19-20, SNAME, pp.15-30.
- Ogilvie, T. F. and Tuck, E. O. (1969). "A rational strip theory for ship motions", *part 1, Report no. 013, Department of Naval Architecture and Marine Engineering, University of Michigan*.
- Salvesen, N.; Tuck, E.O. and Faltinsen, O. (1970). "Ship motion and sea loads". *SNAME Trans*, v.78, pp.1-30.
- Santos, T.A., Winkle, I.E. and Soares, C. Guedes (2002). "Time domain modelling of the transient asymmetric flooding of Ro-Ro ships", *J Ocean Engineering* v.29, pp.667-688.
- Ursell, F. (1949). "On the heaving motion of a circular cylinder on the surface of a fluid", *J Mechanics and Applied Mathematics* v.2, pp.218-31

Lloyd's Register, its affiliates and subsidiaries and their respective officers, employees or agents are, individually and collectively, referred to in this clause as the 'Lloyd's Register Group'. The Lloyd's Register Group assumes no responsibility and shall not be liable to any person for any loss, damage or expense caused by reliance on the information or advice in this document or howsoever provided, unless that person has signed a contract with the relevant Lloyd's Register Group entity for the provision of this information or advice and in that case any responsibility or liability is exclusively on the terms and conditions set out in that contract.